Research Square

Preprints are preliminary reports that have not undergone peer review.
They should not be considered conclusive, used to inform clinical practice,
or referenced by the media as validated information.

Genome-Wide Association Mapping Identifies QTLs for Yield Components under Heat Stress and Cold Tolerance during Seedling Establishment in Mung Bean (Vigna radiata)

Orrasa Aesomnuek
Kasetsart University
Wanchana Aesomnuk
Rice Science Center
Burin Thunnom
National Science and Technology Development Agency
Wasin Poncheewin
National Science and Technology Development Agency
Vinitchan Ruanjaichon
National Science and Technology Development Agency
Kularb Laosatit
Kasetsart University
Prakit Somta
Kasetsart University
Siwaret Arikit
Kasetsart University
Samart Wanchana
samart.wan@biotec.or.th

National Science and Technology Development Agency

Research Article

Keywords: Vigna radiata, heat stress, yield components, cold tolerance, seedling establishment, quantitative trait loci, genome-wide association mapping, FarmCPU, allelic-effect analysis, marker-assisted selection

Posted Date: November 4th, 2026

DOI: https://doi.org/10.21203/rs.3.rs-11377125/v1

License: This work is licensed under a Creative Commons Attribution 4.0 International License.
Read Full License

Additional Declarations: No competing interests reported.

Abstract

Background.

Heat stress during reproductive development and cold stress during seedling establishment are major constraints on mung bean (*Vigna radiata* L. Wilczek) production. However, the quantitative trait loci (QTLs) underlying yield stability under heat stress and cold tolerance during seedling establishment remain largely unknown. A diversity panel comprising 126 mung bean accessions was evaluated for responses to heat and cold stress. Heat-stress responses were quantified as reductions in pod length and seed number per pod relative to control conditions. Cold tolerance during seedling establishment was assessed using germination rate, seedling vigor, and a visual chilling-injury score. Genome-wide association mapping was performed using the multi-locus FarmCPU model, stress-response phenotypes, and 710,906 high-quality single-nucleotide polymorphisms anchored to the JL7 reference genome. Allelic-effect analyses were subsequently conducted for each lead locus to distinguish robust QTLs associated with common alleles from potentially unreliable rare-allele associations.

Results.

QTLs associated with heat-stress responses and cold tolerance were located in distinct genomic regions. A major QTL controlling pod-length reduction under heat stress was identified on chromosome 3 and was consistently detected under two independent heat-stress regimes. This stable heat-tolerance QTL was associated with a common allele that had a large phenotypic effect. Two stable QTLs associated with common alleles were identified for cold tolerance during seedling establishment: one for seedling vigor under cold stress on chromosome 7 at 2.69 Mb and another for chilling-injury score on chromosome 6 at 19.87 Mb. These QTL regions contained biologically plausible candidate genes, including a gene encoding an FKBP62-type immunophilin co-chaperone within the chromosome 3 heat-tolerance QTL and genes encoding the CBF/DREB1 regulator CAMTA5 and a DnaJ/Hsp40 co-chaperone within the chromosome 7 cold-tolerance QTL.

Conclusions.

Genome-wide association mapping combined with allelic-effect validation identified stable QTLs associated with yield components under heat stress and cold tolerance during seedling establishment in mung bean. The heat- and cold-tolerance QTLs were genomically independent, indicating that pyramiding distinct loci will be necessary to combine tolerance to both stresses. These QTLs, particularly those associated with common alleles, represent promising targets for marker-assisted breeding of climate-resilient mung bean cultivars.

Background

Mung bean (*Vigna radiata* L. Wilczek) is an important warm-season, short-duration grain legume crop in Asia. It is an important source of inexpensive, easily digestible dietary protein (20–25% of seed dry weight) and micronutrients and folate [1]. Mung bean is a self-pollinated diploid plant (2n = 2x = 22) with a small genome of approximately 494–579 Mb and a short life cycle of 60 to 75 days [2, 3]. It is well suited for intercropping, catch cropping, and green manuring in cereal-based cropping systems and can form a symbiotic association with rhizobia to fix atmospheric nitrogen to improve soil fertility [1, 2]. As a result, it has been introduced beyond its traditional Asian growing regions into Africa, Australia, and the Americas as a climate-smart pulse crop [2]. While mung bean offers great potential for climate-resilient agriculture, it remains relatively under-researched [4, 5].

The combined effects of rising mean and extreme temperatures, fluctuating rainfall patterns, and shifting agricultural frontiers into cooler and saline lands pose additional challenges to mung bean adaptation and production under climate change [2, 6]. Temperature extremes during the reproductive stage of crops are particularly challenging because they coincide with critical phases of yield formation, including flowering and pod set, in many grain legumes, including mung bean [2]. Developing mung bean cultivars with improved tolerance to heat and cold stress will be essential for maintaining stable production under a changing climate.

The optimum temperature for mung bean growth is 28 to 30°C, and temperatures above approximately 40/28°C (day/night) during the reproductive phase are harmful [1, 7]. During the reproductive stage, heat stress induces flower abscission, pod abortion and reduced pod set, which are associated with impaired reproductive functions, including reduced pollen viability and germination, poor anther dehiscence, decreased pollen load on the stigma, reduced stigma receptivity and impaired pollen-tube growth. These effects, in turn, reduce yield by producing fewer and shorter pods and a lower number of seeds per pod [1, 7, 8]. Pod length and seed number are important yield-associated traits in mungbean; therefore, maintaining these traits under high-temperature conditions may provide useful selection criteria for improving yield performance under heat stress [8, 9]. By contrast, mung bean is a warm-season crop adapted to tropical and subtropical environments but is highly susceptible to low temperatures, particularly during germination and early seedling establishment [10, 11]. Cold reduces germination and early seedling survival, thereby limiting early-season sowing and cultivation at high altitudes and latitudes [11]. Transcriptome analyses have shown distinct expression patterns between low-temperature tolerant and low-temperature susceptible genotypes [10, 11]. Improving the ability of plants to establish under cool conditions broadens the environmental range for mung bean cultivation and expands the area available for growth, thereby complementing efforts to increase heat tolerance.

Both heat stress tolerance and cold stress tolerance share common molecular mechanisms, and candidate genes can be identifed a priori for each mechanism, making these traits tractable targets for genetic mapping. Heat stress tolerance is mediated by heat shock transcription factors, particularly Heat Shock Transcription Factors A1 (HSFA1) and HSFA2, which activate the expression of heat shock proteins. These proteins function as molecular chaperones and protect the proteome during heat stress [12]. Chilling and freezing tolerance are regulated primarily by the ICE1-CBF/DREB1 transcriptional

module, which controls the expression of COLD-REGULATED (COR) genes during cold acclimation [13]. Genomic regions that coincide with these mechanisms are biologically more plausible candidates for association with tolerance.

The declining cost of whole-genome resequencing has made dense, genome-wide marker datasets increasingly accessible for non-model legumes [14, 15]. In combination with genome-wide association studies (GWAS) in diversity panels, it can make used of historical recombination events and high levels of allelic diversity, which may allow more fine-scale mapping than traditional bi-parental linkage analysis [16, 17]. The power to detect polygenic traits can be increased by multilocus models such as FarmCPU, which account for population structure and reduce false positive associations [18]. Mung bean GWAS is beginning to identify loci that control phenological, seed quality, agronomic, and drought related traits [14, 15, 19, 20]. However, explicit QTLs for heat and cold tolerance, based on control versus stress comparisons and validated through allele effect analysis to distinguish strong common variant loci from fragile rare allele artifacts, are not yet available. It remains unclear whether tolerance to these two temperature extremes is governed by shared or independent genetic control, which would determine whether they can be improved jointly or must be pyramided.

In this study, we investigated the genetic architecture of tolerance to contrasting temperature extremes in a diversity panel of 126 *Vigna radiata* accessions. Heat- and cold-response phenotypes were subjected to genome-wide association analysis. For each associated locus, allele frequencies and phenotypic effects were further examined to assess the robustness and breeding relevance of the detected signals. By comparing the loci associated with heat and cold responses, we sought to determine whether adaptation to these contrasting stresses is governed by shared genetic factors or largely independent mechanisms. This study provides a genetic framework for developing mung bean cultivars with greater resilience in an increasingly variable thermal environment.

Results

Variation and repeatability of tolerance phenotypes

The 126 mung bean accessions exhibited wide and continuous variation in their responses to both heat and cold stress (Table 1, Fig. 1). Under heat stress, pod length decreased by an average of 1.3 cm in regime 1 (R1), when stress was imposed during the reproductive stage, and 3.0 cm in regime 2 (R2), when stress was imposed throughout plant development. The corresponding mean reduction in seed number per pod were 2.2 and 5.0 seeds, respectively. Responses varied substantially among accessions, ranging from little or no reduction to severe declines in both traits. The reduction in pod length and seed number per pod were moderately correlated between the two regimes ($r = 0.61$ and 0.56, respectively), indicating moderately repeatable genotypic differences in heat response. Cold-response phenotypes were similary variable. The germination rate under cold conditions ranged from 26.7% to 100%, seedling vigor index from 126 to 695, and cold-injury score from 1.0 to 7.7. Overall, the panel displayed broad,

continuously distributed phenotypic variation in both heat- and cold-stress responses, with no clear separation into discrete response classes.

Table 1
Heat- and cold-response phenotypes used for GWAS analysis

Stress	Tolerance phenotype	N	Mean ± SD	Range	r (R1–R2)
Heat	Pod-length reduction, R1 (cm)	106	1.32 ± 1.06	−1.33–4.70	0.612
Heat	Pod-length reduction, R2 (cm)	107	3.00 ± 1.09	0.71–6.81	0.612
Heat	Seeds-per-pod reduction, R1	105	2.24 ± 1.48	−1.62–5.45	0.561
Heat	Seeds-per-pod reduction, R2	107	5.04 ± 1.84	−6.13–8.37	0.561
Cold	Cold germination rate (%)	110	86.5 ± 13.2	26.7–100	—
Cold	Cold seedling vigor	110	433 ± 114	126–695	—
Cold	Cold injury score (avg)	121	3.34 ± 1.72	1.0–7.67	—

Population structure and linkage disequilibrium

Principal component analysis (PCA) showed continuous genetic variation among the 126 accessions, without clearly separated groups (Fig. 2). The first three principal components accounted for 18.5%, 11.2%, and 4.9% of the total genetic variance, respectively, explaining 34.6% cummulatively (Fig. 2A). K-mean analysis partitioned the accessions into four groups (K = 4), although substantial overlap was observed among them in the PCA space (Fig. 2B). Linkage disequilibrium (LD), estimated separately for each of the 11 chromosomes, declined to half of its maximum value over distances ranging from approximately 155 to 359 kb, with a mean of 257 kb (Fig. 2C). The shortest decay distance was observed on chromosome 11 (approximately 155 kb), whereas the longest was observed on chromosome 7 (approximately 359 kb). A total of 710,906 SNPs were retained for subsequent genome-wide association analyses.

GWAS reveals a reproducible heat-tolerance QTL on chromosome 3

Genome-wide association analyses of the four heat-response indices identified 59 suggestive associations ($-\log_{10}P \geq 4.0$) on several chromosomes (Table 2; Table S1; Fig. 3A). For pod-length reduction, associations were detected within the same region of chromosome 3 in both heat stress regimes. In regime 1, three SNPs were identified, with the strongest association at Chr3:4.50 Mb ($-\log_{10}P = 4.93$; MAF = 0.278). In regime 2, three SNPs were detected approximately 0.4 Mb away, with the peak association at Chr3:4.12 Mb ($-\log_{10}P = 5.52$; MAF = 0.308). Both sets of SNPs were located within the same QTL (approximately 4-Mb on chromosome 3), making this the only region associated with a heat-response index in both stress regimes.

Associations for seeds-per-pod reduction were more widely distributed and differed between regimes. Regime 1 identified 23 suggestive SNPs, including a peak on chromosome 8 at Chr8:14.10 Mb ($-\log_{10}P = 4.14$; MAF = 0.161). In regime 2, 491 suggestive SNPs were detected, most of which were located within a single LD block on chromosome 7, with the strongest association at Chr7:25.45 Mb ($-\log_{10}P = 6.83$). An additional peak was detected on chromosome 1 at Chr1:36.37 Mb ($-\log_{10}P = 6.38$). The peak variants at the chromosome 7 and chromosome 1 loci had minor allele frequencies of ≤ 0.05.

To distinguish loci associated with constitutive trait variation from those associated with heat response, GWAS was also performed separately for each yield component measured under control and heat-stress conditions, without expressing the phenotype as a control-minus-stress reduction. The loci identified from these single-condition traits partially overlapped those detected using the reduction indices. Seeds per pod under control conditions mapped to the same approximately 25-Mb region of chromosome 7 detected for the seeds-per-pod reduction index, together with an additional peak on chromosome 8 at Chr8:34.97 Mb ($-\log_{10}P = 6.53$; Fig. S1). Pod length under heat stress showed its strongest association on chromosome 7 at Chr7:5.24 Mb ($-\log_{10}P = 5.31$; Fig. S1; Table S5). The occurrence of the approximately 25-Mb chromosome 7 signal for both control seed number and heat-induced seed-number reduction indicates that this association may be influenced by constitutive variation in seed number rather than exclusively by the response to heat. Consequently, this region was not prioritized as a heat-response locus. Comparison of the single-condition and reduction-based analyses therefore helped distinguish loci potentially associated with baseline performance from those more specifically associated with heat-induced phenotypic change.

Allelic effects were subsequently examined for the chromosome 3 and chromosome 8 candidate loci (Fig. 3B). At the chromosome 3 locus, accessions carrying the C allele (n = 73) had a mean heat-induced reduction in pod length of 2.5 cm, compared with 4.0 cm among accessions carrying the T allele (n = 32; MAF = 0.31), corresponding to a 62% greater reduction in the T-allele group ($P = 8.6 \times 10^{-9}$). At the chromosome 8 locus, accessions carrying the T allele (n = 16; MAF = 0.16) showed a 56% greater reduction in seeds per pod than those carrying the A allele (n = 87; $P = 2.4 \times 10^{-5}$). Thus, the more frequent alleles at these loci, C on chromosome 3 and A on chromosome 8, were associated with smaller heat-induced reductions in the respective traits.

Table 2
Heat- and cold-tolerance QTLs (FarmCPU, −log10p ≥ 4.0), with their LD blocks and candidate genes from the JL7 functional annotation.

Trait (QTL)	Lead SNP	−log10P	MAF	LD interval (size)	Candidate gene	Class
(Heat) pod-length reduction	Chr3:4.12 / 4.50 Mb	5.52 / 4.93	0.31	3.90–4.75 Mb (848 kb)	FKBP62-type peptidyl-prolyl isomerase (jg7796); WRKY transcription factor 70 (jg7823); NHL-domain protein (jg7813)	Reproducible, robust
(Heat) seeds-per-pod reduction (R1)	Chr8:14.10 Mb	4.14	0.16	13.87–14.34 Mb (471 kb)	Uncharacterised protein (jg37089)	Common
(Heat) Seeds-per-pod reduction (R2)	Chr7:25.45 Mb	6.83	0.02	25.42–25.70 Mb (281 kb)	Probable sulfate transporter 3.3 (jg22407)	Rare allele †
(Heat) Seeds-per-pod reduction (R2)	Chr1:36.37 Mb	6.38	0.05	—	Unannotated model (jg15930)	Rare allele †
(Cold) Seedling vigor	Chr7:2.69 Mb	5.31	0.20	2.45–2.94 Mb (490 kb)	Calmodulin-binding transcription activator 5, CAMTA5 (jg20030); chaperone protein DnaJ 49 / Hsp40 (jg20005); ethylene-responsive TF RAP2-3, AP2/ERF (jg20000); FCS-like zinc-finger 15 (jg19977)	Robust, common
(Cold) Injury score (Chr6)	Chr6:19.87 Mb	4.34	0.28	lead SNP within gene	FAR1-related sequence 9 transcription factor (jg17961; lead SNP inside)	Robust, common
(Cold) Germination rate (Chr6)	Chr6:27.77 Mb	6.52	0.03	27.54–27.77 Mb (232 kb)	Cysteine proteinase RD21A (jg18784); peroxidase 45 (jg18781); myb-like protein (jg18786)	Rare allele †, FDR

Trait (QTL)	Lead SNP	−log10P	MAF	LD interval (size)	Candidate gene	Class
(Cold) Germination rate (Chr11)	Chr11:29.37 Mb	6.11	0.03	—	Unannotated model (jg35830; lead SNP inside)	Rare allele † (n = 1)

GWAS identifies common-allele loci for cold-response traits and model-dependent associations with germination

Genome-wide association analyses of the four chilling-response traits identified 19 suggestive SNP associations (Tables 2 and S1; Fig. 4). Cold seedling vigor showed the most concentrated association signal, consisting of an 11-SNP block spanning 2.68–2.70 Mb on chromosome 7. The lead SNP was located at Chr7:2.69 Mb ($-\log_{10}P = 5.31$; MAF = 0.20) within *jg20018* (Fig. 4A; Table 2). Cold germination showed the strongest individual associations, represented by three SNPs on chromosomes 6 and 11. The lead SNP was located at Chr6:27.77 Mb ($-\log_{10}P = 6.52$), but its minor allele was present at a low frequency (MAF = 0.031; Fig. 4B; Table 2). Cold-injury score was associated with two SNPs on chromosome 6, with the lead SNP at Chr6:19.87 Mb ($-\log_{10}P = 4.34$; MAF = 0.276) located within *jg17961* (Fig. 4C; Table 2). Three additional SNPs associated with seedling height under cold conditions were detected on chromosome 3, led by a SNP at Chr3:24.03 Mb ($-\log_{10}P = 4.40$; MAF = 0.081; Fig. S2, Table S1) .

Allelic effects were examined for the seedling-vigor locus on chromosome 7 and the chilling-injury locus on chromosome 6, both of which had relatively common alleles and lead SNPs located within annotated genes. At Chr7:2.69 Mb, accessions carrying the T allele had greater seedling vigor under cold conditions than those carrying the C allele. At Chr6:19.87 Mb, the A allele was associated with lower chilling-injury scores than the G allele (Fig. 4D). In contrast, the leading SNPs associated with cold germination at Chr6:27.77 Mb and Chr11:29.37 Mb had minor allele frequencies of approximately 0.03 and were represented by only a few accessions (Fig. S3).

Because cold germination rate is a bounded, strongly left-skewed phenotype, with many accessions at the 100% ceiling, and its strongest FarmCPU associations rested on rare alleles, we suspected that the skew was inflating these low-frequency signals. To test this, the germination values were logit-transformed and re-analysed with a principal-component-controlled single-locus model. This scan recovered 50 SNPs at FDR < 0.05, with only modest residual genomic inflation ($\lambda = 1.15$). The strongest association now fell in a common-variant region at approximately 18 Mb on chromosome 1, whereas support for the previously leading rare-allele SNP at Chr6:27.77 Mb dropped to $-\log_{10}P = 3.04$ (Fig. S4). The cold-germination signals therefore shifted with both phenotype transformation and the way population structure was modelled, indicating that the rare-allele germination peaks are sensitive to analytical choices and should be interpreted with caution.

Candidate genes within LD-defined intervals

Candidate intervals were defined using SNPs in local linkage disequilibrium with each lead SNP ($r^2 \geq 0.2$), and genes located within these intervals were identified using the JL7 functional annotation (Table 2; complete gene lists are provided in Table S4). The reproducible locus on chromosome 3 associated with heat-induced pod-length reduction was located within an approximately 848-kb LD block spanning 3.90–4.75 Mb. This interval was shared between the two experimental regimes and contained 60 annotated genes, including a WRKY70-like transcription factor (*jg7823*), an FKBP62-like immunophilin co-chaperone (*jg7796*), and several leucine-rich repeat receptor-like kinases. The chromosome 7 interval associated with seedling vigor under cold conditions spanned 2.45–2.94 Mb and contained 74 genes. These included a DnaJ/Hsp40 co-chaperone (*jg20005*), a RAP2-3-like AP2/ERF transcription factor (*jg20000*), an FCS-like zinc-finger protein (*jg19977*), and a CAMTA5-like calmodulin-binding transcription activator (*jg20030*). The lead SNP at Chr7:2.69 Mb was located within an uncharacterized gene model, *jg20018*.

At the chromosome 6 locus associated with cold-injury score, the lead SNP was located within a FAR1-related transcription-factor gene (*jg17961*). Local LD surrounding this SNP was limited, and no extended candidate interval was defined. The chromosome 6 interval associated with cold germination contained a class III peroxidase gene annotated as *Peroxidase 45* (*jg18781*), a MYB-like transcription-factor gene (*jg18786*), and a responsive-to-dehydration cysteine-protease gene annotated as *RD21A* (*jg18784*). Screening the LD-defined intervals against predefined temperature-stress-related gene families therefore identified co-chaperones and transcriptional regulators within both the heat- and cold-response intervals.

Discussion

To our knowledge, this is the first genome-wide SNP-based association study to map QTLs for yield components under heat stress and cold tolerance during seedling establishment in mung bean using stress-response phenotypes. Three findings are central. First, the reduction in pod length under heat stress identified a QTL on chromosome 3, which was detected in two independent heat regimes. Second, cold tolerance yielded two common-allele QTLs, one for seedling vigor on chromosome 7 and one for cold-injury score on chromosome 6. Third, several of the statistically strongest association peaks were rare-allele artifacts. The heat- and cold-associated loci mapped to non-overlapping genomic regions, indicating that the two temperature tolerances are under largely independent genetic control.

Genetic diversity, population structure and linkage disequilibrium of the panel

The panel exhibited continuous rather than discrete genetic differentiation. Principal component analysis resolved a gradient along the first three components, rather than distinct clusters. K-means partitioning produced only loosely defined groups and model-based ancestry analysis likewise indicated substantial admixture [21]. Weak, clinal structure of this kind is advantageous for association mapping because it reduces spurious genotype-phenotype correlations caused by strong stratification and because a small

number of principal components, three in the present analysis, is sufficient to account for the remaining structure [22]. All tolerance phenotypes segregated broadly and, in several cases, transgressively, providing the phenotypic variation needed to detect common-allele QTLs of moderate effect in a panel of this size.

Genome-wide linkage disequilibrium (LD) decayed to half of its maximum value at approximately 257 kb, an extended decay distance that is consistent with the predominantly autogamous mating system of mung bean [19]. Two practical implications follow. First, the 710,906 filtered SNPs provide adequate genome coverage, so that when a trait yielded no strong association, the seeds-per-pod reduction index being the clearest example, polygenic control by loci of small effect is a more likely explanation than insufficient marker density. Second, each significant SNP tags a haplotype block of comparable size, so the candidate intervals reported here contain many genes and the resolution for causal-gene identification is inherently limited; narrowing these intervals will require dense local genotyping or QTL-seq in segregating populations [23]. Both observations are consistent with those reported for other *Vigna* and autogamous legume panels and should inform the design of follow-up validation populations [5, 17, 19].

Stress-response phenotypes as the target of mapping

The biological interpretation of a GWAS signal depends on how the stress phenotype is defined. We therefore restricted QTL inference to stress-response phenotypes and excluded traits scored under favorable conditions alone [6, 24]. For heat stress, matched control and stress measurements were available, and the response was expressed as the control-minus-heat reduction in pod length and seed number. For cold stress, no control-subtracted index was computed; instead, direct cold-response phenotypes were mapped, namely germination and seedling vigor under chilling, together with a visual cold-injury score, which are established measures of chilling tolerance. This approach is justified because germination and establishment under warm conditions are nearly uniform across the panel, and because the injury score is, by definition, a damage trait; each therefore reflects the response to low temperature rather than intrinsic plant size.

Both experiments illustrate why performance under stress alone is an unreliable mapping target. The strongest seeds-per-pod association (chromosome 7, ~ 25 Mb) was robust for control seed number but weak for the heat-reduction index, and mapping seed number under heat alone would have led to its interpretation as a heat-tolerance locus. Conversely, the control-only baseline trait, seedling height at normal temperature, yielded no significant SNPs, whereas the cold-response traits did. Although this distinction is long established in stress physiology, it is applied inconsistently in crop GWAS, where performance under stress is frequently mapped without reference to the corresponding response [6]. Our results support adopting reduction indices where a control is available, or direct injury and recovery scores where it is not, as the primary mapping target, with single-condition values retained for biological interpretation. This approach is conservative, in that strong but uninformative signals are excluded, but it increases the likelihood that a reported locus reflects tolerance per se and is transferable across

environments. One caveat should be noted: seedling vigor under colde retains some component of intrinsic vigor, whereas the cold-injury score, as a direct damage measure, is the least confounded of the cold traits and germination rate is the most closely anchored to a control.

A reproducible heat-tolerance QTL on chromosome 3

The pod-length reduction QTL on chromosome 3, spanning approximately 4 Mb, is the most robust finding of this study. It was detected in both experimental rounds and is associated with a common allele of large effect (MAF 0.26 to 0.31), with the susceptible allele increasing heat-induced pod-length loss by 62 to 130%. Reproducibility across environments is the most stringent criterion for distinguishing true QTLs from background noise in stress mapping, because genotype-by-environment interaction and phenotyping error together increase regime-specific false positives [24]. A region that recurs across independent regimes, segregates at moderate allele frequency, and affects a yield component directly is, on these grounds, the strongest candidate for marker development among the loci identified here.

Findings in related legumes are consistent with this interpretation. Stable genomic regions for pod and seed set under heat have been reported in chickpea, and multiple loci for reproductive heat-response traits in cowpea, indicating that these traits are genetically tractable [6, 25, 26]. Pod length under heat depends on the maintenance of pollination, fertilization, and early pod development, all of which are heat-sensitive steps in mung bean [7, 8]; the chromosome 3 interval therefore warrants screening for genes involved in pollen and pod development, as well as for canonical thermotolerance regulators such as heat-shock factors and heat-shock proteins [12]. Identification of the causal gene within the approximately 257 kb LD block will require fine-mapping and functional analysis.

Common-allele QTLs for cold tolerance

Two common-allele QTLs for cold tolerance were statistically robust and biologically interpretable. The chromosome 7 locus (2.69 Mb) reduced seedling vigor under chilling by approximately 20% and was supported by a coherent cluster of 11 SNPs. The chromosome 6 locus (19.87 Mb), with its lead SNP located within a gene model, reduced the visible cold-injury score by 42%, indicating that the minor allele confers tolerance. Together, these loci combine moderate allele frequency with robust, PC-adjusted effects, meeting the criteria for a practical selection marker.

Cold tolerance at germination and at the seedling stage has a well-characterized regulatory basis in the ICE1–CBF/DREB1 cascade and its downstream COR genes, which provides strong candidate genes for these intervals [13]. Comparable resources exist in other crops: SNPs and candidate genes associated with cold tolerance at germination have been identified in soybean [27], and major seedling cold-tolerance QTLs with validated candidate genes have been fine-mapped in rice [28]. The loci reported here extend this work to a tropical legume in which the genetics of cold tolerance have been little explored, and they define specific intervals for targeted candidate-gene screening.

Robustness of common- versus rare-allele associations

A methodological observation emerges from these results: the statistically strongest association is not necessarily the most informative. The FDR-significant cold-germination signals on chromosomes 6 and 11 depended on alleles carried by only one to three accessions. The chromosome 6 peak decreased from −log10(P) = 6.52 to 3.04 when the strongly skewed germination phenotype was logit-transformed and reanalyzed, and the leading signal shifted to a common-variant region on chromosome 1. Rare alleles, together with non-normal phenotype distributions, are a well-recognized source of inflated and poorly reproducible associations [29].

Grouping accessions by genotype at each lead SNP and reporting per-allele sample sizes allowed allele-effect analysis to distinguish these unstable signals from the robust common-allele QTLs, providing a straightforward safeguard that appears in relatively few studies. We therefore recommend that crop GWAS report minor-allele counts at lead SNPs as standard practice, assess the sensitivity of results to phenotype transformation, and prioritize common-allele loci for marker development, while reserving rare-allele signals for validation in larger or purpose-enriched panels. The modest inflation observed in the transformed single-locus scan (λ = 1.15) further indicates that the transformed cold-germination phenotype should be reanalyzed with a kinship-controlled, multilocus model before any germination locus is treated as definitive.

Independent genetic architecture and implications for breeding

The heat- and cold-associated loci occupied distinct genomic regions, with no lead SNPs shared within ± 100 kb. Chromosome 7, the only chromosome carrying loci for both stresses, contained them at widely separated positions. No pleiotropic multi-stress locus was detected, indicating that the two tolerances are inherited largely independently and that combining them will require pyramiding distinct loci rather than selecting a single region [30]. This finding is directly applicable. The chromosome 3 heat QTL and the chromosome 6 and 7 cold QTLs are each moderate-frequency common alleles with direct effects on tolerance traits, so each can be tagged with a co-dominant marker and stacked in elite backgrounds. This approach remains underused in mung bean despite the expanding genomic resources available for the crop [25], and together these loci could subsequently support genomic selection models for temperature resilience [31]. The broader workflow is also transferable. It includes mapping tolerance from stress-response phenotypes, validating lead signals through allele effect analysis, and distinguishing common from rare alleles. These steps are applicable to other stresses and to crops targeted for climate adaptation [2].

Candidate genes within the QTL intervals

Functional annotation of the JL7 gene models enabled us to move beyond gene identifiers and to ask whether the canonical temperature-stress pathways were represented within the QTL intervals. The chromosome 7 chilling-vigor block contains CAMTA5, a calmodulin-binding transcription activator that binds the CM2 promoter motif of CBF/DREB1 genes and activates them during cold acclimation, thereby linking calcium signaling to the freezing-tolerance transcriptome [13, 32, 33], as well as a DnaJ/Hsp40

co-chaperone [34], a well-established upstream regulator of the cold-response cascade, located within a validated cold-tolerance QTL. The reproducible chromosome 3 heat QTL contains an FKBP62-type immunophilin, an HSP90-associated co-chaperone linked to thermotolerance [12, 35], adjacent to a tandem cluster of WRKY70 transcription factors, and the cold-germination QTL contains a responsive-to-dehydration protease (RD21A) [36] and a class III peroxidase [37], consistent with dehydration-stress signaling and with the control of reactive oxygen species during germination. These gene families are those expected a priori to underlie heat and cold tolerance [12, 13], and their presence beneath the association peaks strengthens support for the loci. These findings should nevertheless be interpreted cautiously because the LD blocks span up to approximately 850 kb and contain dozens of genes; therefore, the proposed candidates require further evaluation through fine-mapping, haplotype analysis, and gene-expression studies.

Limitations and future directions

Several limitations qualify these conclusions. The phenotyped panel was modest in size, with approximately 110 to 121 accessions per trait, which limited statistical power and the detection of loci with small effects; most associations were suggestive rather than genome-wide significant; and the extended linkage disequilibrium characteristic of an autogamous species, with a half-decay distance of approximately 257 kb, means that each association tags a large, gene-rich haplotype block. Phenotyping was conducted at a single facility for each temperature treatment, limiting our ability to assess genotype-by-environment interactions. However, the two heat regimes, together with the requirement that a signal be reproducible across both regimes, reduce this limitation for the chromosome 3 QTL. Future work should therefore focus on expanding the panel, conducting multi-environment trials, fine-mapping the priority QTLs and completing functional annotation for the three common-allele loci. Together, these steps would move these QTLs from discovery toward deployment in climate-resilient mung bean cultivars.

Conclusions

Using stress-response phenotypes, we mapped heat- and cold-tolerance QTLs in a 126-accession mung bean panel and validated them by allele-effect analysis. A reproducible chromosome 3 QTL governs heat-induced pod-length loss, and two common-allele QTLs on chromosomes 7 and 6 control cold seedling vigor and cold injury; several headline peaks, including the FDR cold-germination signals, proved to be fragile rare-allele artefacts. Heat and cold QTLs are genomically independent, so combining the two tolerances will require pyramiding distinct loci. These validated, common-allele QTLs are immediate targets for marker-assisted breeding of climate-resilient mung bean.

Methods

Plant material and diversity panel

A panel of 126 mung bean (*V. radiata*) accessions, drawn from the germplasm collection maintained at Department of Agronomy, Faculty of Agriculture at Kamphaeng Saen, Kasetsart University, Thailand, to represent landraces and improved cultivars of diverse geographic origin, was evaluated for heat and cold tolerance and whole-genome sequenced (Table S6). Stress-screening trials followed a completely randomised design with three replicates; the heat assay was conducted in two heat regimes (R1, R2). Association analyses used the 105–121 accessions with complete data for each trait.

Tolerance phenotyping and definition of comparison traits

Heat tolerance was evaluated by comparing control and heat-treated plants under two independent heat regimes that differed in the timing and duration of heat exposure. In the first regime, heat was imposed only at the reproductive stage: at flowering, half of each accession's pots were moved into a heat greenhouse for the duration of the heat treatment, while the remaining pots were kept in an ambient greenhouse as the matched control. In the second regime, heat was imposed throughout the life cycle, with plants grown in the heat greenhouse from sowing to maturity alongside a matched set of control plants in the ambient greenhouse. Both heat greenhouses were equipped with WatchDog microclimate loggers, and in each regime the heat treatment consisted of day temperatures of 40 to 45°C for 6 h, from 10:00 to 16:00, and night temperatures of 28 to 30°C, with 50 to 60% relative humidity and approximately 761 μmol m^{-2} s^{-1} PAR (Fig. S5). Pod length and seeds per pod were recorded under both control and heat conditions in each regime, and the tolerance index was defined as the heat-induced reduction in each trait, calculated as control minus heat. Thus, a smaller reduction indicated greater tolerance. Cold tolerance was assessed at two stages. For germination, trays were maintained at 15°C and compared with a 25°C control, and responses were scored as germination rate at 8 days and seedling vigor index (SVI = % germination × hypocotyl length) [38]. For seedling chilling, 14-day-old seedlings were exposed to 15°C for 21 days and scored on a 1 to 9 cold-injury scale, where 1 indicated the most tolerant response and 9 the most susceptible response; the scores were averaged as Cold_Score_Mean. Each stage included ten seeds or seedlings per accession in three replicates. Phenotypic distributions, descriptive statistics, and between-regime repeatability, defined as the Pearson correlation of a trait across the two heat regimes, were computed in R.

DNA extraction, whole-genome resequencing and variant calling

Genomic DNA was extracted from young leaves using the DNeasy 96 Plant Kit (QIAGEN) and whole-genome resequenced with short-read next-generation sequencing (DNBSeq T7). The reads were aligned to the *V. radiata* Jilv7 (JL7) chromosome-scale reference assembly [39], and SNPs and InDels were called using the GATK best-practices pipeline [40]. More than 2.7 million raw SNPs were identified and filtered to retain bi-allelic, non-heterozygous sites with minor allele frequency (MAF) ≥ 0.05 and missing rate ≤ 20%, yielding 710,906 high-quality SNPs for association analysis.

GWAS analysis

Association analysis was conducted using the multi-locus Fixed and random model Circulating Probability Unification (FarmCPU) model [18], implemented in GAPIT (v3) [41]. The first three principal components (PC1 to PC3) were included as covariates to control for population structure [22], and marker filtering criteria of MAF ≥ 0.05 and missing rate ≤ 20% were applied. Significance was assessed at three levels: a Bonferroni genome-wide threshold ($\alpha = 0.05$), a Benjamini-Hochberg false-discovery rate [42] (FDR < 0.05), and a suggestive threshold of $-\log_{10}p \geq 4.0$ for reporting. Lead SNPs detected in the same LD block across the two experimental regimes were treated as reproducible QTLs, and each QTL is reported by its lead SNP rather than by the number of correlated SNPs within the LD block.

Allele-effect analysis and robustness checks

Each lead SNP was dissected by grouping accessions by genotype and testing the effect on the tolerance phenotype by ordinary least squares with adjustment for population structure (phenotype ~ allele + PC1 + PC2 + PC3); the additive allele effect, its p-value, the percentage difference between allele classes and the per-allele sample size were recorded. Loci whose minor allele was carried by ≤ 3 (up to 5) accessions were flagged as fragile rare-variant signals. Because cold germination rate was left-skewed with a ceiling at 100%, it was logit-transformed [43] and re-scanned by a PC-controlled single-locus model; the genomic-inflation factor (λ) and BH-FDR were recomputed to test the robustness of its associations to phenotype distribution and model choice. Allele-effect and robustness analyses were performed in R.

Candidate gene identification and functional annotation

For each lead SNP the local LD block was defined empirically as the contiguous span of SNPs in $r^2 \geq 0.2$ with the lead SNP, estimated from the 126-accession genotype matrix, and all gene models overlapping this interval were retrieved from the JL7 annotation. Putative functions were assigned from the JL7 functional annotation, which integrates homology to UniProt/SwissProt and NCBI non-redundant (nr) proteins with Pfam, InterPro, Gene Ontology, KEGG and eggNOG domain assignments. Candidate genes were prioritised by stress-relevant function and every block was additionally screened against the canonical thermotolerance (*HSP*/*HSF*, chaperones/co-chaperones) and cold-tolerance (*CBF/DREB–ICE1–COR*, *CAMTA* regulators, *RD/LEA* dehydration genes) gene families.

Declarations

Ethics approval and consent to participate

Not applicable.

Consent for publication

Not applicable.

Competing interests

The authors declare that they have no competing interests.

Funding

We are thankful to the National Science, Research and Innovation Fund, Thailand Science Research and Innovation (TSRI) (Grant No.: FFB680075/0337) for funding the project.

Author Contribution

S.W., P.S., S.A. conceived the study; O.A. performed phenotyping; W.A., W.P. and B.T. performed bioinformatics and GWAS; O.A., S.W. drafted the manuscript; S.W., V.R., and K.L. reviewed the manuscript. All authors read and approved the final manuscript.

Acknowledgement

We would like to thank the Department of Agronomy, Faculty of Agriculture at Kamphaeng Saen, Kasetsart University, for providing the mung bean germplasm used in this study. We also thank the Rice Science Center for providing the facilities used for phenotyping.

Data Availability

The raw sequencing data generated in this study have been deposited in the NCBI Sequence Read Archive (SRA) under accession number PRJNA1543770.

References

1. HanumanthaRao B, Nair RM, Nayyar H. Salinity and High Temperature Tolerance in Mungbean [Vigna radiata (L.) Wilczek] from a Physiological Perspective. Front Plant Sci. 2016;7:957.
2. Considine MJ, Siddique KHM, Foyer CH. Nature’s pulse power: legumes, food security and climate change. J Exp Bot. 2017;68:1815–8.
3. Oraon PK, Ambreen H, Yadav P, Ramarao S, Goel S. A chromosome-scale reference assembly of Vigna radiata enables delineation of centromeres and telomeres. Sci Data. 2025;12:305.
4. Somta P, Laosatit K, Yuan X, Chen X. Thirty years of mungbean genome research: where do we stand and what have we learned? Front Plant Sci. 2022;13:944721.
5. Kim SK, Nair RM, Lee J, Lee S-H. Genomic resources in mungbean for future breeding programs. Front Plant Sci. 2015;6:626.

6. Sita K, Sehgal A, HanumanthaRao B, Nair RM, Vara Prasad PV, Kumar S, et al. Food legumes and rising temperatures: effects, adaptive functional mechanisms specific to reproductive growth stage and strategies to improve heat tolerance. Front Plant Sci. 2017;8:1658.
7. Sharma L, Priya M, Bindumadhava H, Nair RM, Nayyar H. Influence of high temperature stress on growth, phenology and yield performance of mungbean [Vigna radiata (L.) Wilczek] under managed growth conditions. Sci Hortic. 2016;213:379–91.
8. Kaur R, Bains TS, Bindumadhava H, Nayyar H. Responses of mungbean (Vigna radiata L.) genotypes to heat stress: Effects on reproductive biology, leaf function and yield traits. Sci Hortic. 2015;197:527–41.
9. Jha UC, Shafi S, Tallury S, Nayyar H, Ciampitti IA, Siddique KHM, et al. Differential physiological and yield responses of selected mung bean (Vigna radiata (L.) R. Wilczek) genotypes to various high-temperature stress regimes. Sci Rep. 2025;15:1034.
10. Chen L-R, Ko C-Y, Folk WR, Lin T-Y. Chilling susceptibility in mungbean varieties is associated with their differentially expressed genes. Bot Stud. 2017;58:7.
11. Manasa LS, Panigrahy M, Panigrahi KC, Mishra G, Panda SK, Rout GR. Cold Tolerance Mechanisms in Mungbean (Vigna radiata L.) Genotypes during Germination. Agriculture. 2023;13:315.
12. Ohama N, Sato H, Shinozaki K, Yamaguchi-Shinozaki K. Transcriptional regulatory network of plant heat stress response. Trends Plant Sci. 2017;22:53–65.
13. Shi Y, Ding Y, Yang S. Molecular regulation of CBF signaling in cold acclimation. Trends Plant Sci. 2018;23:623–37.
14. Han X, Li L, Chen H, Liu L, Sun L, Wang X, et al. Resequencing of 558 Chinese mungbean landraces identifies genetic loci associated with key agronomic traits. Front Plant Sci. 2022;13:1043784.
15. Chang Y, Peng L, Ji L, Wang S, Wang L, Wu J. Genome-wise association study identified genomic regions associated with drought tolerance in mungbean (Vigna radiata (L.) R. Wilczek). Theor Appl Genet. 2023;136:40.
16. Korte A, Farlow A. The advantages and limitations of trait analysis with GWAS: a review. Plant Methods. 2013;9:29.
17. Noble TJ, Tao Y, Mace ES, Williams B, Jordan DR, Douglas CA, et al. Characterization of linkage disequilibrium and population structure in a mungbean diversity panel. Front Plant Sci. 2017;8:2102.
18. Liu X, Huang M, Fan B, Buckler ES, Zhang Z. Iterative Usage of Fixed and Random Effect Models for Powerful and Efficient Genome-Wide Association Studies. PLoS Genet. 2016;12:e1005767.
19. Sokolkova A, Burlyaeva M, Valiannikova T, Vishnyakova M, Schafleitner R, Lee C-R, et al. Genome-wide association study in accessions of the mini-core collection of mungbean (Vigna radiata) from the World Vegetable Gene Bank (Taiwan). BMC Plant Biol. 2020;20(Suppl 1):363.
20. Breria CM, Hsieh CH, Yen J-Y, Nair R, Lin C-Y, Huang S-M, et al. Population Structure of the World Vegetable Center Mungbean Mini Core Collection and Genome-Wide Association Mapping of Loci Associated with Variation of Seed Coat Luster. Trop Plant Biol. 2020;13:1–12.

21. Alexander DH, Novembre J, Lange K. Fast model-based estimation of ancestry in unrelated individuals. Genome Res. 2009;19:1655–64.
22. Price AL, Patterson NJ, Plenge RM, Weinblatt ME, Shadick NA, Reich D. Principal components analysis corrects for stratification in genome-wide association studies. Nat Genet. 2006;38:904–9.
23. Takagi H, Abe A, Yoshida K, Kosugi S, Natsume S, Mitsuoka C, et al. QTL-seq: rapid mapping of quantitative trait loci in rice by whole genome resequencing of DNA from two bulked populations. Plant J. 2013;74:174–83.
24. Fischer RA, Maurer R. Drought resistance in spring wheat cultivars. I. Grain yield responses. Aust J Agric Res. 1978;29:897–912.
25. Paul PJ, Samineni S, Thudi M, Sajja SB, Rathore A, Das RR et al. Molecular mapping of qtls for heat tolerance in chickpea. Int J Mol Sci. 2018;19.
26. Lucas MR, Ehlers JD, Huynh B-L, Diop N-N, Roberts PA, Close TJ. Markers for breeding heat-tolerant cowpea. Mol Breed. 2013;31:529–36.
27. Chen Y, Liu Z, Han D, Yang Q, Li C, Shi X, et al. Cold tolerance SNPs and candidate gene mining in the soybean germination stage based on genome-wide association analysis. Theor Appl Genet. 2024;137:178.
28. Yang L, Wang J, Han Z, Lei L, Liu HL, Zheng H, et al. Combining QTL-seq and linkage mapping to fine map a candidate gene in qCTS6 for cold tolerance at the seedling stage in rice. BMC Plant Biol. 2021;21:278.
29. Tabangin ME, Woo JG, Martin LJ. The effect of minor allele frequency on the likelihood of obtaining false positives. BMC Proc. 2009;3 Suppl 7:S41.
30. Dormatey R, Sun C, Ali K, Coulter JA, Bi Z, Bai J. Gene Pyramiding for Sustainable Crop Improvement against Biotic and Abiotic Stresses. Agronomy. 2020;10:1255.
31. Crossa J, Pérez-Rodríguez P, Cuevas J, Montesinos-López O, Jarquín D, de Los Campos G, et al. Genomic selection in plant breeding: methods, models, and perspectives. Trends Plant Sci. 2017;22:961–75.
32. Kidokoro S, Yoneda K, Takasaki H, Takahashi F, Shinozaki K, Yamaguchi-Shinozaki K. Different Cold-Signaling Pathways Function in the Responses to Rapid and Gradual Decreases in Temperature. Plant Cell. 2017;29:760–74.
33. Doherty CJ, Van Buskirk HA, Myers SJ, Thomashow MF. Roles for Arabidopsis CAMTA transcription factors in cold-regulated gene expression and freezing tolerance. Plant Cell. 2009;21:972–84.
34. Kong F, Deng Y, Zhou B, Wang G, Wang Y, Meng Q. A chloroplast-targeted DnaJ protein contributes to maintenance of photosystem II under chilling stress. J Exp Bot. 2014;65:143–58.
35. Meiri D, Breiman A. Arabidopsis ROF1 (FKBP62) modulates thermotolerance by interacting with HSP90.1 and affecting the accumulation of HsfA2-regulated sHSPs. Plant J. 2009;59:387–99.
36. Koizumi M, Yamaguchi-Shinozaki K, Tsuji H, Shinozaki K. Structure and expression of two genes that encode distinct drought-inducible cysteine proteinases in Arabidopsis thaliana. Gene.

1993;129:175–82.

37. Passardi F, Cosio C, Penel C, Dunand C. Peroxidases have more functions than a Swiss army knife. Plant Cell Rep. 2005;24:255–65.
38. Abdul-Baki AA, Anderson JD. Vigor determination in soybean seed by multiple criteria[1]. Crop Sci. 1973;13:630–3.
39. Liu C, Wang Y, Peng J, Fan B, Xu D, Wu J, et al. High-quality genome assembly and pan-genome studies facilitate genetic discovery in mung bean and its improvement. Plant Commun. 2022;3:100352.
40. Van der Auwera GA, Carneiro MO, Hartl C, Poplin R, Del Angel G, Levy-Moonshine A et al. From FastQ data to high confidence variant calls: the Genome Analysis Toolkit best practices pipeline. Curr Protoc Bioinformatics. 2013;11:11.10.1–11.10.33.
41. Wang J, Zhang Z. GAPIT version 3: boosting power and accuracy for genomic association and prediction. Genomics Proteom Bioinf. 2021;19:629–40.
42. Benjamini Y, Hochberg Y. Controlling the false discovery rate: a practical and powerful approach to multiple testing. J Roy Stat Soc: Ser B (Methodol). 1995;57:289–300.
43. Warton DI, Hui FKC. The arcsine is asinine: the analysis of proportions in ecology. Ecology. 2011;92:3–10.

Figures

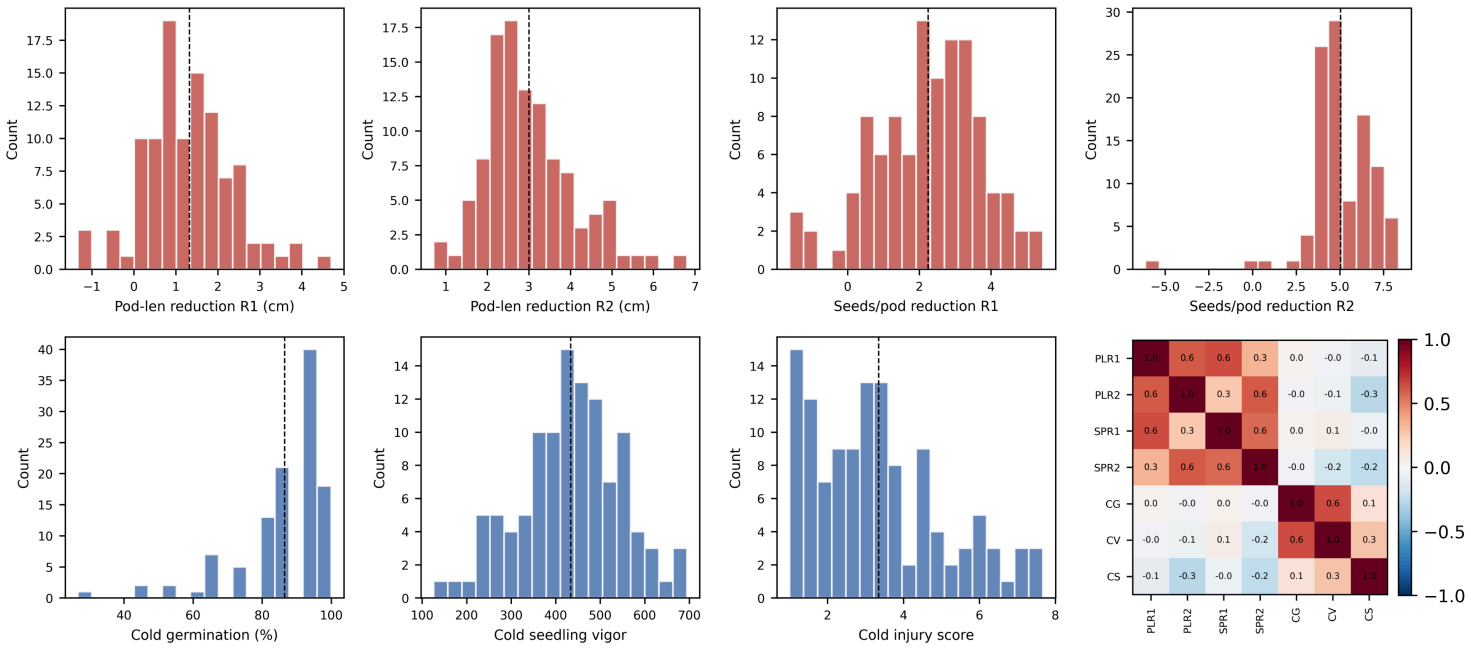


Figure 1

Phenotypic variation in the heat- and cold-tolerance indices. Histograms show the four heat-reduction indices and three cold-response traits (dashed line = mean); the lower-right panel is the pairwise

correlation among indices, showing that heat traits correlate among themselves (r ≈ 0.3–0.6) while heat–cold correlations are near zero. PLR, pod-length reduction; SPR, seeds-per-pod reduction; CG, cold germination; CV, cold seedling vigor; CS, cold injury score.

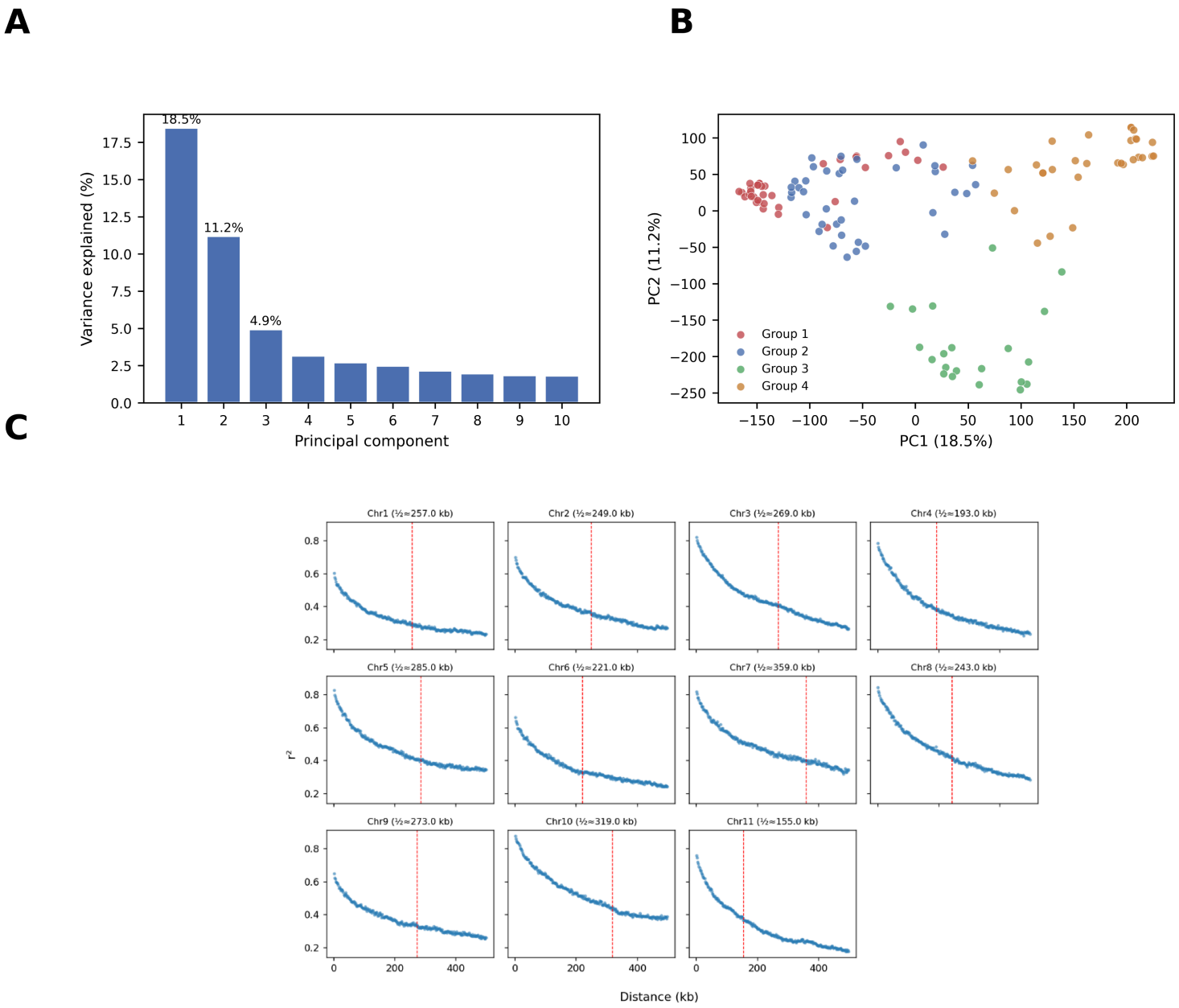


Figure 2

Population structure and linkage disequilibrium of the 126-accession GWAS panel. (A) Proportion of genetic variance explained by the first ten principal components (PC1–PC3 = 18.5%, 11.2%, 4.9%). (B) PCA on PC1–PC2, accessions coloured by k-means group (K = 4). (C) LD decay analysed separately for each of the 11 chromosomes (mean half-decay ~257 kb; range 155 kb on chromosome 11 to 359 kb on chromosome 7).

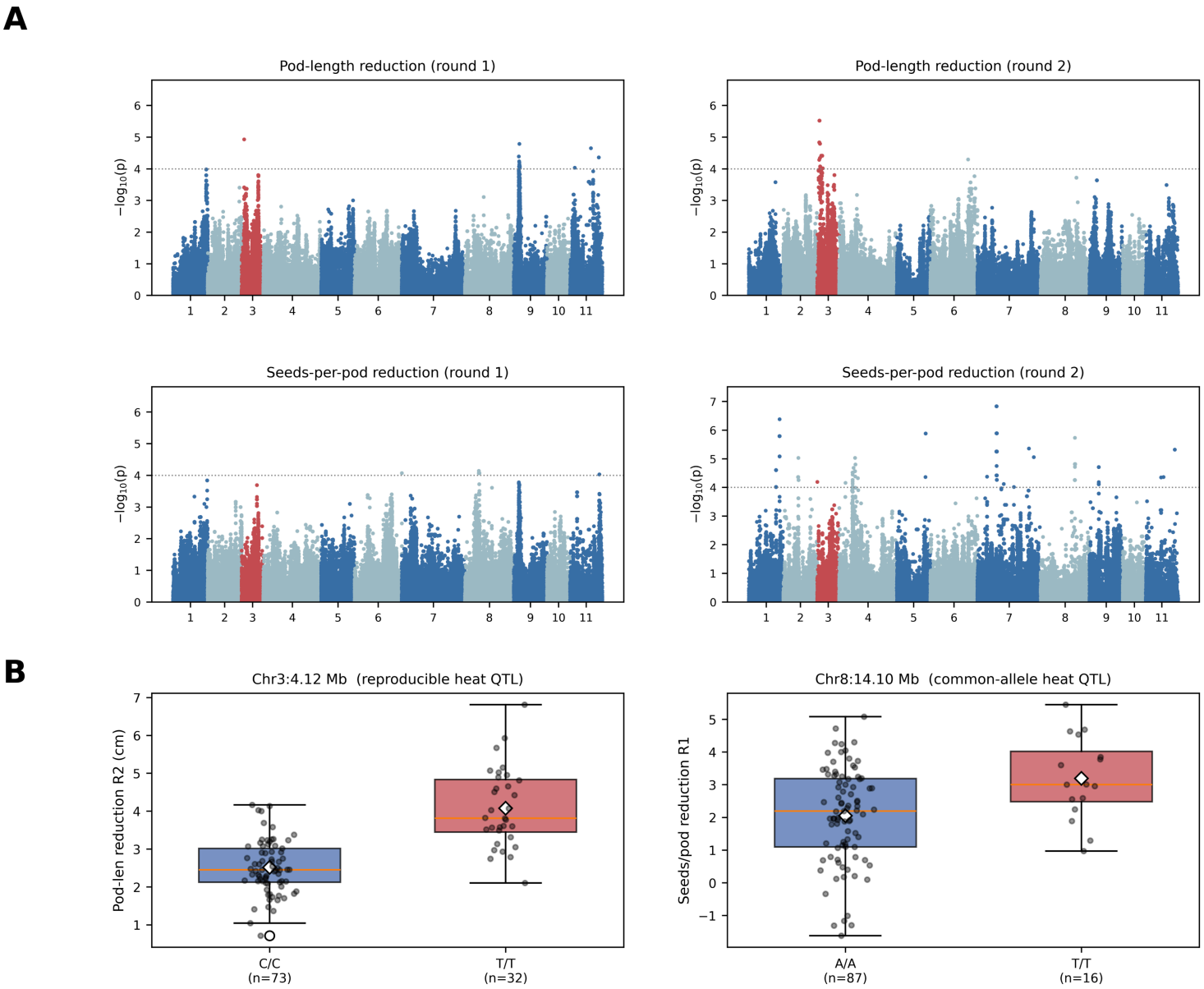


Figure 3

Heat-tolerance QTLs from control–stress reduction indices. (A) Manhattan plots of the four heat-reduction indices; chromosome 3 (red) carries a pod-length-reduction QTL reproducible across both rounds (dotted line, −log10p = 4.0). (B) Allelic effects at the common-allele heat QTLs (Chr3:4.12 Mb, MAF 0.31, reproducible; Chr8:14.1 Mb, MAF 0.16); the minor allele increases stress-induced loss. Diamonds = means.

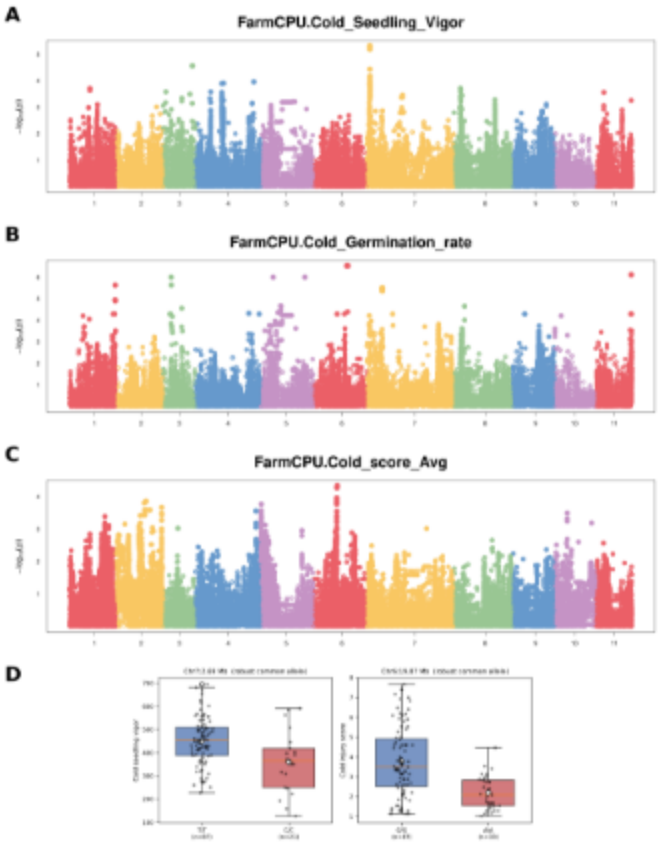


Figure 4

Cold-tolerance QTLs. (A) Manhattan plot for cold seedling vigor (11-SNP block on chromosome 7, 2.68–2.70 Mb). (B) Manhattan plot for cold germination rate (peaks on Chr6/Chr11, rare alleles). (C) Manhattan plot for cold-injury score (lead SNP Chr6:19.87 Mb, −log10p = 4.34, within jg17961). (D) Allelic effects at the two robust common-allele cold QTLs, the seedling-vigor locus (Chr7:2.69 Mb) and the cold-injury locus (Chr6:19.87 Mb), contrasted with the fragile rare-allele germination peak (Chr6:27.77 Mb, n = 3). Boxes show the two homozygous genotype classes; the white diamond marks the mean and the orange line the median.

Supplementary Files

This is a list of supplementary files associated with this preprint. Click to download.

- Additionalfile1.xlsx
- Additionalfile2.pdf